Physica Medica 59 (2019) 133–141

Contents lists available at ScienceDirect

Physica Medica

journal homepage: www.elsevier.com/locate/ejmp

Original paper

Skin DVHs predict cutaneous toxicity in Head and Neck Cancer patients treated with Tomotherapy

M. Mori[a,*], G.M. Cattaneo[a], I. Dell'Oca[b], S. Foti[b], R. Calandrino[a], N.G. Di Muzio[b], C. Fiorino[a]

[a] Medical Physics, San Raffaele Scientific Institute, Milan, Italy
[b] Radiotherapy, San Raffaele Scientific Institute, Milan, Italy

ARTICLE INFO

Keywords:
Head and Neck Cancer
Skin dose
IMRT
Predictive models
Acute
Skin toxicities

ABSTRACT

Purpose: To explore the association between planning skin dose-volume data and acute cutaneous toxicity after Radio–chemotherapy for Head and Neck (HN) cancer patients.

Methods: Seventy HN patients were treated with Helical Tomotherapy (HT) with radical intent (SIB technique: 54/66 Gy to PTV1/PTV2 in 30fr) ± chemotherapy superficial body layer 2 mm thick (SL2) was delineated on planning CT. CTCAE v4.0 acute skin toxicity data were available. Absolute average Dose-Volume Histograms (DVH) of SL2 were calculated for patients with severe (G3) and severe/moderate (G3/G2) skin acute toxicities.

Differences against patients with none/mild toxicity (G0/G1) were analyzed to define the most discriminative regions of SL2 DVH; univariable and multivariable logistic analyses were performed on DVH values, CTV volume, age, sex, chemotherapy.

Results: Sixty-one % of patients experienced G2/G3 toxicity (rate of G3 = 19%). Differences in skin DVHs were significant in the range 53-68Gy (p-values: 0.005–0.01). V56/V64 were the most predictive parameters for G2/G3 (OR = 1.12, 95%CI = 1.03–1.21, p = 0.001) and G3 (OR = 1.13, 95%CI = 1.01–1.26, p = 0.027) with best cut-off of 7.7cc and 2.7cc respectively. The logistic model for V56 was well calibrated being both, slope and R2, close to 1. Average V64 were 2.2cc and 6cc for the two groups (G3 vs G0-G2 toxicity); the logistic model for V64 was quite well calibrated, with a slope close to 1 and R2 equal to 0.60.

Conclusion: SL2 DVH is associated with the risk of acute skin toxicity. Constraining V64 < 3cc (equivalent to a 4x4cm2 skin surface) should keep the risk of G3 toxicity below or around 10%.

1. Introduction

The modalities of delivering radiotherapy of Head and Neck Cancers (HNC) have changed dramatically in recent decades. Technological developments have allowed a shift from static X-ray beams, often mixed with electron beams, to Intensity Modulated Radiation Therapy (IMRT), and more recently to rotational techniques such as Volumetric Modulated Arc Therapy (VMAT) and Helical TomoTherapy (Accuray, Sunnyvale, CA) (HT). These new techniques, thanks to Image Guidance Radiation Therapy (IGRT) and plan adaptation through Adaptive Radiation Therapy (ART) have contributed to an improvement in loco-regional control and cancer-specific survival by means of a careful 'painting' of the dose distribution around the target volume(s), thereby minimizing the irradiation of the nearby normal structures. Other aspects rendering HNC treatments particularly challenging include the large tumor volumes surrounded by radiosensitive organs, and target location, which normally extends near the patient's skin. IMRT and VMAT are able to obtain optimal target coverage, with higher dose conformity and homogeneity than permitted by simpler conformal techniques, and demonstrate better outcomes in terms of tumor control and normal tissue complication probabilities [1]. On the other hand, RT is still associated with clinically significant side effects [2–8], including the onset of acute skin reactions for patients treated with IMRT [4]; in addition, a recent study showed an increased incidence of acute skin toxicity in HT compared with other IMRT/VMAT techniques [8]. In general, the assessment of dosimetric and clinical predictors of skin toxicity remains poorly investigated, despite being increasingly recognized as a clinically significant issue; skin toxicities often occur in the early phase, sometimes leading to treatment interruption, with a consequent potentially detrimental effect on the therapy. In addition, such toxicities may translate into an increased risk of late fibrosis [9], with persisting/chronic symptoms and, of course, may severely affect the patient's quality of life (QoL) during and immediately after RT [10–14]. All of this evidence suggests the existence of a potential and as

* Corresponding author.
E-mail address: mori.martina@hsr.it (M. Mori).

https://doi.org/10.1016/j.ejmp.2019.02.015
Received 31 July 2018; Received in revised form 13 February 2019; Accepted 15 February 2019
Available online 26 February 2019

yet unexplored benefit from skin sparing techniques, given the continued priority of maintaining sufficiently large margins to avoid tumor missing prior to the current IGRT era and/or to the current lack of adequate tools for "safe" skin sparing during plan optimization. Doses to the skin may change significantly during treatment, due to the complex combination of body contour modifications and the position of the skin relative to the incident fluence patterns, and are also largely dependent on the planning technique and the dimension/shape/position of Clinical Target Volume (CTV)/Planning Target Volume (PTV) with respect to the skin. Investigations into the risk of an increase in skin dose during therapy were previously performed at our institution through the implementation and validation of an internal method for the computation of the "dose-of-the-day" actually delivered to the skin, allowing its evaluation [15–17]. In any case, no information on dose-volume/surface relationships between the dose received by the skin and the insurgence of skin toxicity is currently available, and there are very few works in the literature dealing with the quantitative prediction of skin toxicity in the modern IMRT era [7–9,12–14,18,19]. In this study, performed on a cohort of HNC patients treated with HT at our institution, we attempted to investigate whether the dose received by the skin as calculated in the planning phase is predictive of the risk of acute skin toxicity, with the final aim of quantifying the relationship between such risk and dose-volume parameters. The potential need of skin sparing technique implementation is subsequently discussed.

2. Material and methods

2.1. Patient characteristics

The study involved 70 consecutive patients treated in the period 2007–2017 with a simultaneous integrated boost (SIB) approach delivering 54/66 Gy in 30 fractions to low-risk lymph nodes (PTV1) and tumor/positive lymph nodes (PTV2) respectively with HT (no Cetuximab); for selected patients an additional concomitant boost on FDG-PET positive volumes delivering 69 Gy/30 fraction was also performed. All patients signed a specific informed consent for the use of data and images for research activity. The main patient clinical and dosimetric data are shown in Table 1; staging is reported according to the American Join Committee on Cancer (AJCC) [27]. In total, 51 (73%) were male and 19 (27%) female; mean and median age were 62 and 64 years. The large majority of patients, 54 (77%), received concurrent chemotherapy (CDDP, Cisplatin 100 mg/m^2); no patients received Cetuximab. Eleven patients also received induction chemotherapy following Al-Sarraf or TPF scheme.

Table 1
Summary of main patients' characteristics.

Age (y)	mean, median, range	63, 64, 30–89
Sex	male	51
	female	19
Primary tumor location	Nasopharynx	11
		III (7), n.a. (4)
	Oropharinx	40
		II (10), III (21), n.a. (9)
	Oral cavity	7
		II (5), III (1), n.a. (1)
	Hypopharynx	8
		II (3), III (1), IV (1), n.a. (3)
	nasal-sinus	1
		n.a.
	pharinx	1
		II
	larynx	1
		II (1)
	n.a.	1
		n.a.
Hystology	Spinocellular	53
	Undifferentiated	5
	Lymphoepithelioma	1
	Nasopharynx	9
	Oropharinx	1
	Adenosquamous	1
Chemotherapy	yes	54
	no	14
	missing	2
CTV Volume (cc)	mean, median, range	220, 215, (65.7–461.8)
Acute Tox grade	G0/G1, G2, G3	27, 30, 13
V54 (cc)	mean, median, range	16.3, 14.1, (0.9–53.5)
V56 (cc)	mean, median, range	11.1, 8.9, (0–42.2)
V58 (cc)	mean, median, range	8.6, 6.6, (0–38.5)
V60 (cc)	mean, median, range	6.6, 4.2, (0–34.8)
V62 (cc)	mean, median, range	4.8, 2.6, (0–30.5)
V64 (cc)	mean, median, range	3, 0.9, (0–26.2)

*n.a.: not available.
*Staging is reported according to American Joint Committee on Cancer (AJCC) criteria.

2.2. Contouring, planning, image-guidance procedures

Details of contouring, planning optimization and image-guidance procedures have been described elsewhere [20–22] and are here briefly summarized. For radical patients, the RT protocol used at our institute consists of a SIB approach [22]; all patients were planned on PET/CT images. Two clinical target volumes (CTVs) were defined: CTV1, including the regional nodes at risk according to published criteria for selection and delineation of the neck nodes [23], and CTV2, including the tumour plus positive lymph nodes. Each CTV was expanded to the PTV (5-mm margin). In case the PTV extended outside the body it was cropped with a margin of 0–2 mm from the body surface, as established by the physician. The SIB approach was planned and delivered with the intent to concomitantly deliver 54 Gy and 66 Gy in 30 fractions to PTV1 and PTV2 respectively. For several patients an additional concomitant boost on Fluoro-Deoxy-Glucose-Positron Emission Tomography (FDG-PET) positive volumes delivering 69 Gy/30 fraction was also performed [22]. Regarding Organ At Risk (OARs), the parotids, mandible (including the temporo-mandibular joint), optic structures, brain, brain stem, and spinal cord were contoured, with the last two automatically expanded (5–8 mm) to generate the corresponding spinal cord and brain stem PRV (Planning Risk Volume). A number of other structures were also defined, including the mucosa outside the PTVs, larynx, thyroid, inner ear, esophagus, lung apexes, vertebral body and submental connective tissue. Regarding planning optimization, the criteria for target structures and OAR objectives were assessed in part according to the Radiation Therapy Oncology Group protocol H-0022 [24], and in part according to the experience of Eisbruch et al. [25] as well as our own institute. The greatest priority was given to PTV coverage and spinal cord, brain stem and visual pathway constraints, which are considered "hard constraints", i.e. those which must be satisfied even at the expense of PTV coverage. Many "soft" constraints were then applied, with an "as low as reasonably achievable" approach was followed for most OARs (e.g. parotids, oral cavity and larynx). Our approach was shown to be highly efficient, providing high homogeneity of both the dose distribution within PTV and the PTV coverage, and an optimal sparing of OARs [21,22,26].

A field dimension of 2.5 cm, modulation factor of 2.5–3, and pitch of 0.287–0.35 were used. All patients were treated with daily image-guidance through MegaVoltage Computed Tomography (MVCT).

2.3. Extraction of skin-dose and available clinical data

All HT plans for the considered patients were recalculated with a fine resolution grid (0.15 × 0.15 cm^2) as required for accurate skin dose calculation due to the steepness of the dose gradient in the build-up region. Plans were optimized by means of the HT TPS (v 5.1.1.6) through dynamic penalized optimization, based on collapse cone

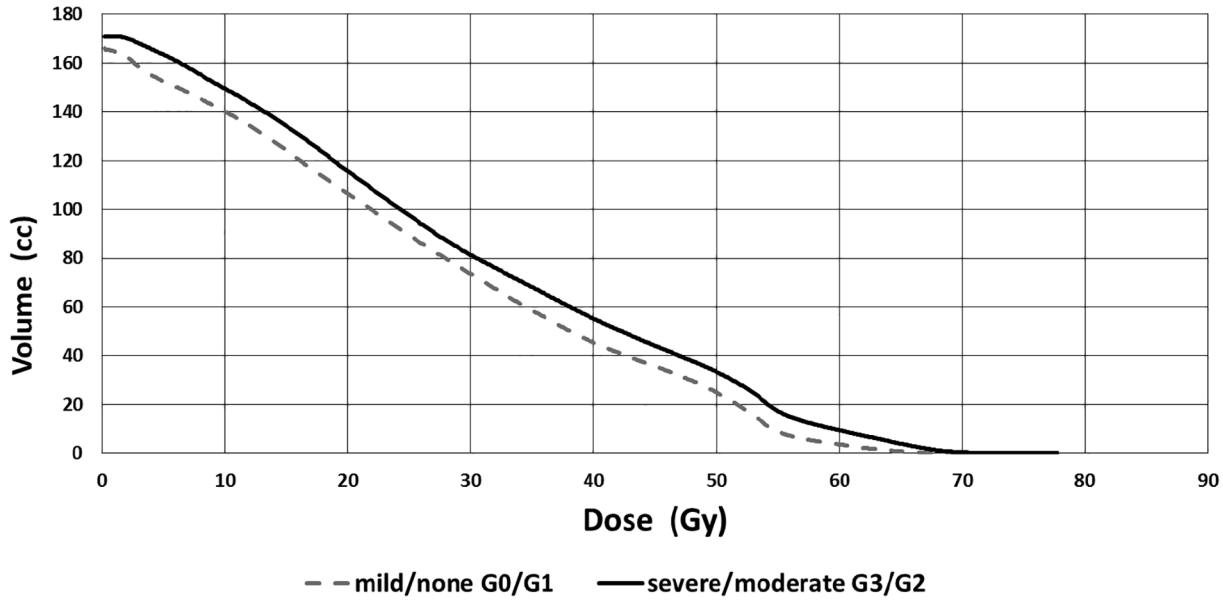

Fig. 1. Average skin DVHs referring to patients experiencing moderate/severe (G3/G2, black solid line) against none/mild (G1/G0, grey dashed line) acute skin toxicity.

convolution algorithms [28,29] and delivered by HT. The reliability of the HT TPS for the dose assessment in both build-up and superficial regions was not investigated in this work, but confirmed by several studies, and the consistency between different HT TPS is guaranteed by the same configuration respect to a gold standard HT TPS. Several studies were performed both in vivo and in phantoms using various detectors with different active volume dimensions and depths of measurement; in general, good agreement between planned and measured data was found, suggesting a sufficient reliability of the HT TPS for the dose assessment in both build-up and superficial regions of several Tomotherapy HN plans, generally within 3–5% [30,31]. A superficial 2 mm thick body layer (SL2) was automatically delineated with a cranial-caudal extension corresponding to the high-dose PTV2 on the planning CT using a commercial software (MIM v. 6.5.5) and considered as a surrogate for the skin. In fact, the epidermal shell is bonded through the basement membrane to the 1–3 mm thick dermal shell. The upper portion is the papillary layer, which contains the micro vessels supplying the epidermis. Since the most frequent acute skin toxicities such as dermatitis and erythema are related to vascularization, a 2 mm thickness was chosen [33,34]. Patients were generally examined before the treatment, once a week during the treatment, at treatment end, and at 3 months after treatment end. According to CTCAE v4.0, acute skin toxicity information was assessed as the peak score recorded during the treatment and after the treatment within 3 months from its end [35].

2.4. Analyses and modeling

Absolute Dose-Volume Histograms (DVH) of SL2 were calculated and average values for patients who developed severe/moderate (G3/G2) and mild/none (G1/G0) skin acute toxicities were assessed. DVH differences were analyzed by two-tailed *t*-test to define the most discriminative regions of SL2 DVH [36]; dose-volume constraints were tentatively suggested. The association with toxicities, first G2/G3 and then only G3, was tested for V54, V56, V58, V60, V62, V64 by univariable logistic analysis: the same variables were entered into a stepwise multivariable logistic regression. The resulting best dosimetry predictor was entered into a backward stepwise multivariable logistic regression together with the available clinical variables (CTV volume, sex, chemotherapy (yes/no) and age). Analyses were performed with MedCalc software (bvba, Brussels, Belgium). The population was divided into quartiles and the parameters of the best overall model fit of both scenarios were used to design the curve and to build the calibration plot. Goodness of fit was determined by the Hosmer-Lemeshow (HL) test, considering acceptable goodness of fit when $p > 0.05$ [37]. The calibration plot of the resulting logistic model was built: observations were grouped into equi-interval bins (quartiles), and the predicted probability of the event was plotted against the proportion of actual events within each group.

2.5. Impact of dose calculation uncertainty

Dose calculation uncertainty in the first few mm from body surface is known to be affected by relatively large uncertainty [30–32]. In order to quantify the potential impact of this uncertainty on the results of the logistic regressions, we performed a sensitivity analysis: we focused on G3 toxicities since it is the less robust scenario in terms of number of events. A gaussian probability dose error distribution with a constant SD in the range 50–70 Gy was first considered to represent random inter-patient dose uncertainty (note that any systematic error would not impact on the association between DVH and toxicity). A value of 5% for the inter-patient SD of the dose error was safely adopted, being reasonably larger than values mostly reported in literature [30,31]. Then, the original DVHs were randomly modified by applying the mentioned gaussian probability distribution, obtaining a modified population incorporating dose uncertainty. The process was repeated 200 times as well as the corresponding logistic regression expressing the relationship between the best dosimetric predictor and the risk of G3 toxicity (assessed in the original population). The resulting distributions of p-values and OR referred to the 200 scenarios were considered and compared against the original values to finally estimate the impact of dose uncertainty on the resulting logistic model.

3. Results

3.1. Predictors of G2/G3 skin toxicity

Regarding G2/G3 toxicity, the average DVHs for G2/G3 vs G0/G1 patients are shown in Fig. 1. Sixty-one percent of patients experienced G2/G3 toxicity. As shown by the two tailed *t*-test in Fig. 2, differences in skin DVHs were significant in the range 50–68 Gy, suggesting that the fraction of SL2 receiving around 1.7–2.3 Gy/fr is highly correlated with the risk of skin acute toxicity. In the plateau of the DVH region with

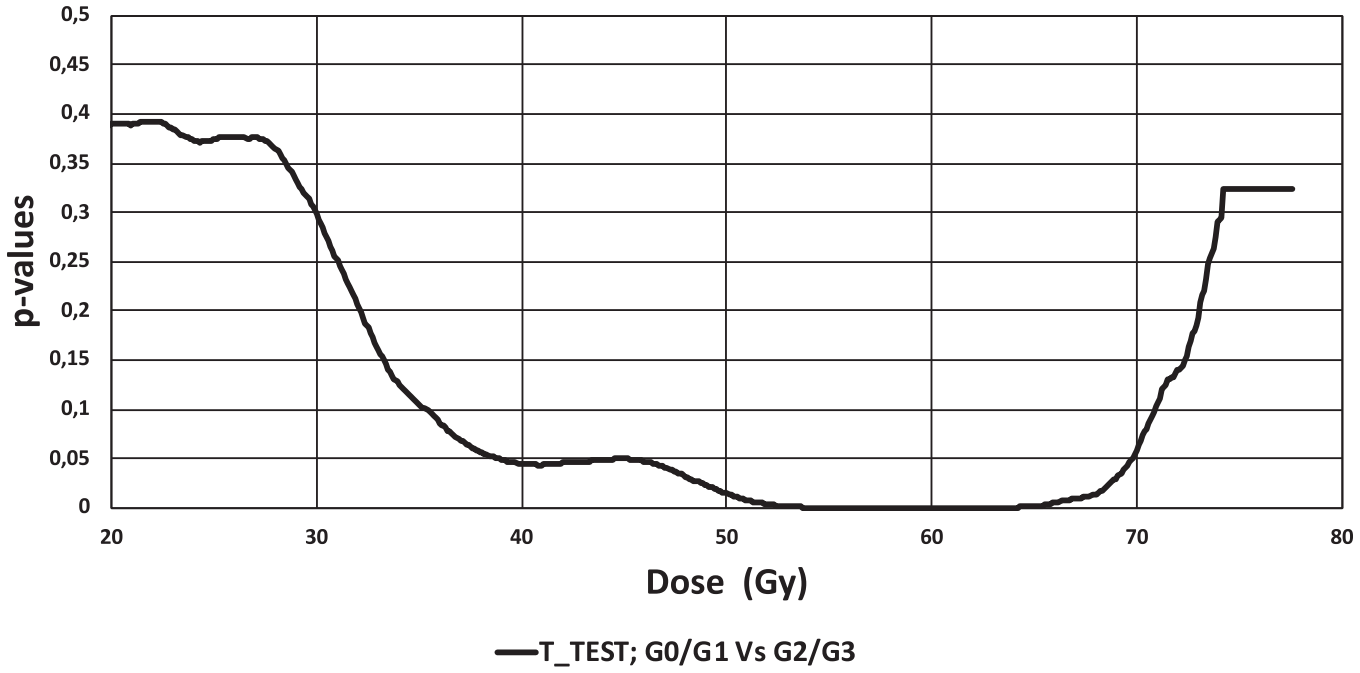

Fig. 2. Results of two-tailed *t*-test p-values of the differences between DVHs shown in Fig. 1 (G3/G2 vs G1/G0 acute skin toxicity).

Table 2
Results of univariable and multivariable logistic analyses for predictors of G2/G3 acute skin toxicity.

Univariable Logistic Regression		Overall Model Fit	Coefficients and Std Errors			Odds Ratios and 95% CL		HL	ROC Analysis	
endpoint: tox G2/G3	Variable	Significant Level	Coefficient	Std. Error	Constant	Odds ratio	95% CI		ROC	95% CL
	V54	P = 0.0015	0.081	0.030	−0.731	1.085	1.023–1.150	P = 0.0879	0.699	0.578–0.803
	V56	P = 0.0007	0.117	0.042	−0.667	1.124	1.036–1.221	P = 0.2580	0.724	0.605–0.824
	V58	P = 0.0005	0.147	0.053	−0.592	1.158	1.043–1.285	P = 0.0140	0.724	0.604–0.824
	V60	P = 0.0005	0.180	0.067	−0.486	1.197	1.049–1.366	P = 0.0106	0.711	0.590–0.813
	V62	P = 0.0003	0.246	0.095	−0.394	1.279	1.062–1.542	P = 0.0881	0.707	0.586–0.810
	V64	P = 0.0004	0.391	0.169	−0.258	1.479	1.063–2.059	P = 0.0364	0.678	0.555–0.785
Multivariable logistic regression		Overall Model Fit	Coefficients and Std Errors			Odds Ratios and 95% CL		HL	ROC Analysis	
endpoint: tox G2/G3	Variable	Significant Level	Coefficient	Std. Error	Constant	Odds ratio	95% CI		ROC	95% CL
V54.V56.V56.V58.V60.V62.V64	V56	P = 0.0007	0.117	0.042	−0.667	1.124	1.036–1.221	P = 0.2580	0.724	0.605–0.824
V56.CTV.SEX.AGE	V56	P = 0.0010	0.112	0.041	−0.662	1.118	1.032–1.212	P = 0.2632	0.715	0.592–0.818

highly significant differences, p-values ranged between 0.005 and 0.01. Results of the univariable and multivariable logistic analyses are shown in Table 2. From univariable logistic regression on dosimetric variables, V56 emerged as the best dosimetric predictor (OR = 1.12, 95%CI = 1.04–1.22, p = 0.0007). V56 was the only independent predictor also when tested by age, sex, chemotherapy and CTV volume, (OR = 1.12, 95%CI = 1.03–1.21, p = 0.001). As reported in Fig. 1 and Table 4, average V56 were 14.5 cc and 6.8 cc for the two groups (i.e. G2/G3 vs G0/G1) with a best-cut-off value of 7.7 cc (AUC = 0.74): the rate of G2/G3 toxicity was 33/41 (80.5%) for V56 ≥ 7.7 cc and 10/29 (34.5%) for V56 < 7.7 cc respectively. Results of V56 logistic regression fitting are reported in Fig. 3, with a comparison of actual and expected events from the model (coefficients of the logistic model β_0 and β_1 were found to be −0.667 and 0.117 respectively); goodness of fit was adequate (HL test, p = 0.26). Fig. 4 shows the optimal performance of the model in terms of calibration, with R^2 and slope both near 1.

3.2. Predictors of G3 skin toxicity

Nineteen percent of patients experienced G3 toxicity; the resulting average DVHs, shown in Fig. 5, did not show a significant region for the two-tailed *t*-test, although two groups were well separated and p-values were of borderline significance (best value 0.09) with a quasi-plateau in the range 54–68 Gy, as shown in Fig. 6. Results of the univariable and multivariable logistic analyses are shown in Table 3. From univariable logistic regression on dosimetric variables, V64 emerged as the best parameter associated with risk of G3 toxicity (OR = 1.13, 95%CI = 1.01–1.26, p = 0.025). V64 was the only independent predictor also from multivariable regression, (OR = 1.13, 95%CI = 1.01–1.26, p = 0.027). Average V64 were 2.2 cc and 6 cc for the two groups (G3 vs G0/G1/G2) with a best cut-off value of 2.7 cc: the rate of G3 toxicity 7/21 (33.3%) for V64 ≥ 2.7 cc and 6/49 (12.2%) for V64 < 2.7 cc respectively (AUC = 0.65). Results of V64 logistic regression fitting are reported in Fig. 7, with the comparison of actual and expected events from the model (coefficients of the logistic model β_0 and β_1 were −1.90 and 0.12 respectively); goodness of fit was acceptable (HL test, p = 0.61). Fig. 8 shows the calibration plot of the model with an R^2 equal to 0.60 and a slope still very close to 1.

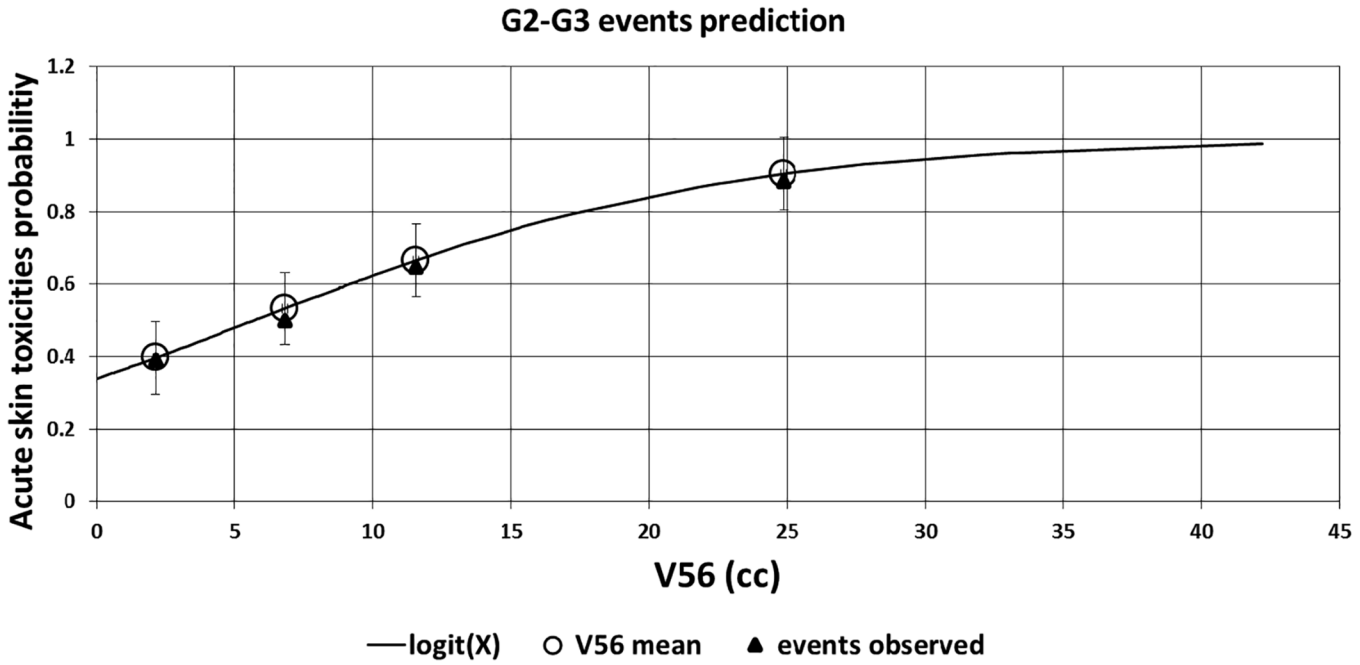

Fig. 3. Logistic plot of the relationship between V56 (resulting as the most predictive DVH parameter) of SL2 and the risk of G2/G3 acute skin toxicity. Triangles show the true rates grouped for each quartile, while the circles show the predicted values with their confidence intervals.

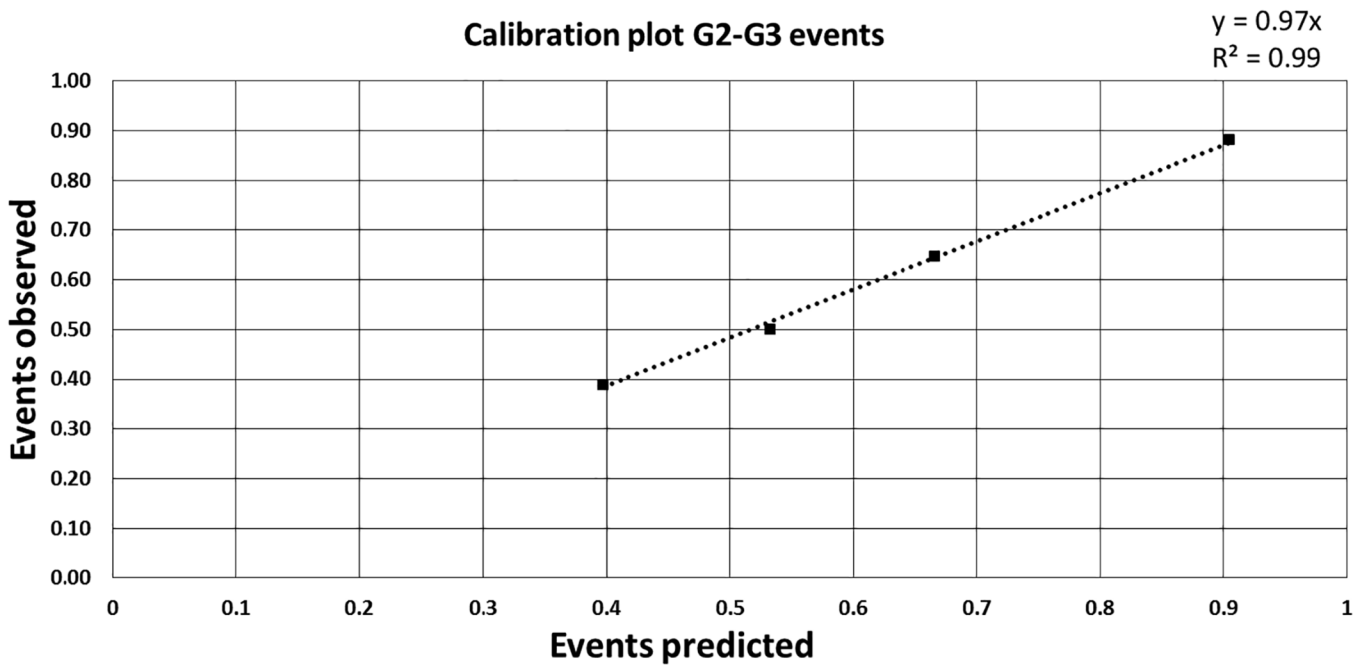

Fig. 4. Calibration plot of the logistic model of Fig. 3 for G2/G3 acute skin toxicity.

3.3. Impact of dose uncertainty on modeling

Results of DVH resampling of the original population showed that dose uncertainty has negligible impact on the association between V64 and G3 toxicity: the inter-quartile range of the resulting distribution of p-values was 0.018–0.033 (mean value: 0.025) against an original value equal to 0.025; similarly the inter-quartile range of ORs was 1.13–1.14 (mean value: 1.13) against an original value equal to 1.13. The impact of including dose uncertainty was also small for the coefficients of the corresponding logistic regressions (i.e.: variations within few %).

4. Discussion and conclusion

In this work the skin dose-surface relationship for HNC patients treated with SIB delivered with a daily dose of 2.2 Gy/fr to the high dose PTV using HT was quantified for the first time. Despite the relatively small number of patients, the results clearly showed that the DVH of SL2 was highly associated with the risk of developing acute skin toxicity after HT. The resulting models for the prediction of acute skin toxicities were accurate in prediction, and that for G2/G3 toxicities was highly exact. Very interestingly, despite the limited number of events, a clear relationship was also found for the more clinically significant G3 toxicities. The most important result emerging from this work is that

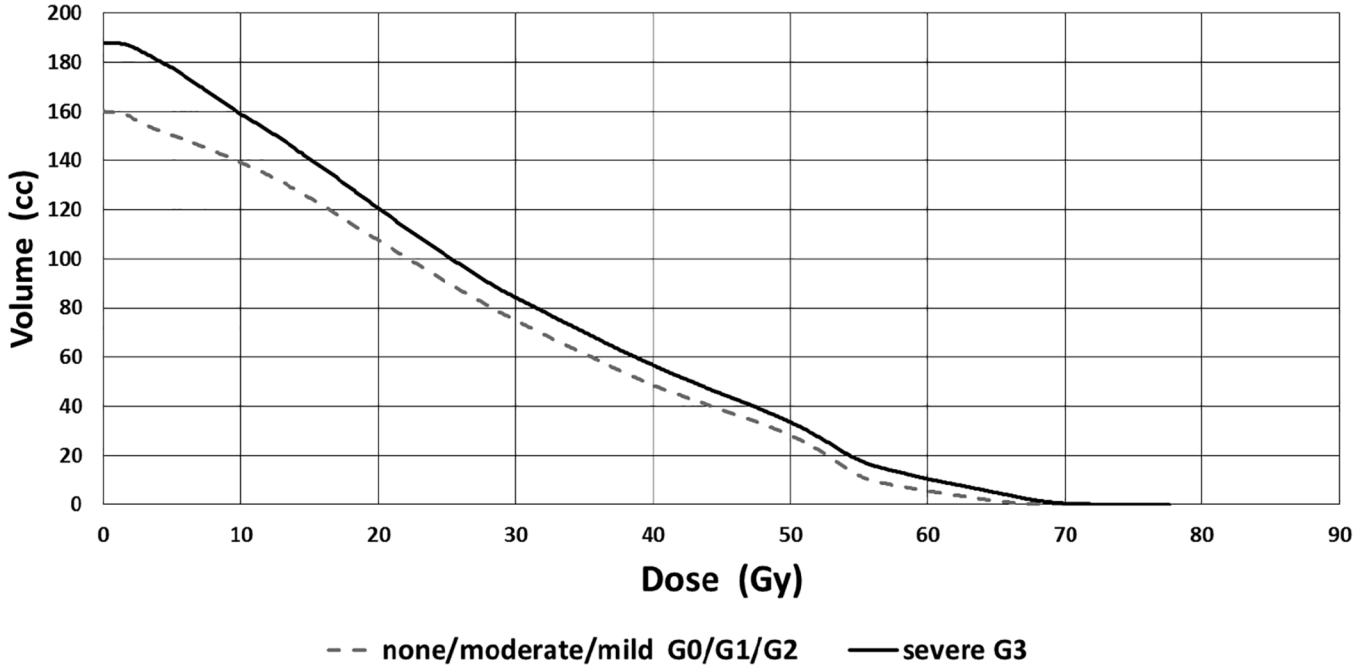

Fig. 5. Average skin DVHs referring to patients experiencing severe (G3, black solid line) against none to moderate (G0-G2, grey dashed line) acute skin toxicity.

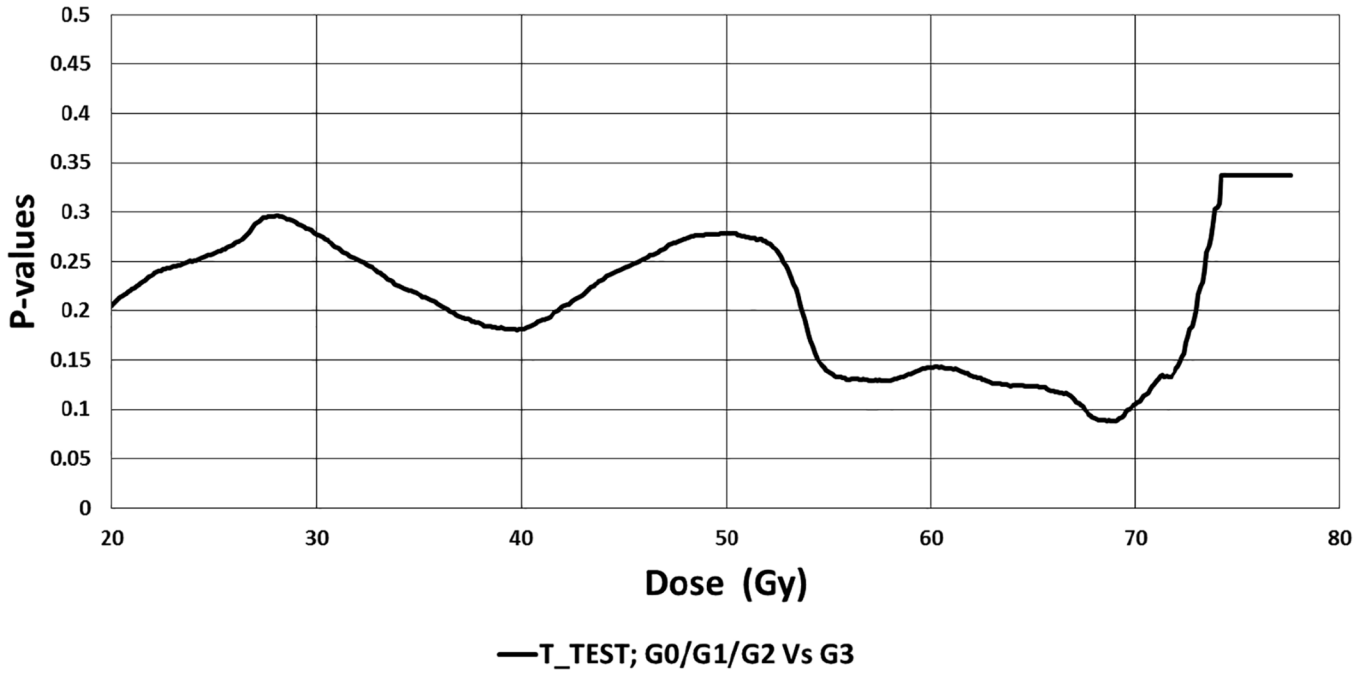

Fig. 6. Results of two-tailed *t*-test p-values of the differences between DVHs shown in Fig. 5 (G3 vs G0-G2 acute skin toxicity).

the entire range of high doses from around 54–64 Gy is clearly associated with the risk of skin toxicity. In terms of the best cut-off values potentially usable as constraints during planning optimization, limiting V56 below approximately 8 cc (corresponding to 40 cm^2, slightly more than a 6x6 cm^2 square surface) should keep the risk of G2/G3 toxicities around 30%. Regarding G3 toxicities the trend was confirmed, although the false positive rate increased (as shown in Table 4), likely due to the small number of events. Results showed that limiting V64 < 3 cc (15 cm^2, approximately equal to a 4x4 cm^2 square surface) should keep the risk level at around 10% with an increasing risk above 30% for values around 8–10 cc. These results could be applied during the planning phase: once the SL2 DVH has been calculated, the radiation oncologist could predict the individual patient risk of skin toxicity and decide accordingly whether to reduce the dose to the skin. In this case, of course, care should first be taken to avoid increasing the risk of missing the target during treatment, which could prove challenging in many situations. This can help the clinician in planning a specific and individually optimized medication program during and after the therapy, aiming to prevent the effects and/or reducing their severity.

Several factors have previously been reported as predictors of the risk of acute effects to the skin, such as the presence of psoriasis [38] and diabetes [39]. Allergy, hypertension and long-term smoking are associated with a significant increase in risk of telangiectasia [40]. In addition, several drugs are known to increase the radiosensitivity of the

Table 3
Results of univariable and multivariable logistic analyses for predictors of G3 acute skin toxicity.

Univariable Logistic Regression		Overall Model Fit	Coefficients and Std Errors			Odds Ratios and 95% CL		HL	ROC Analysis	
endpoint: tox G3	Variable	Significant Level	Coefficient	Std. Error	Constant	Odds ratio	95% CI		ROC	95% CL
	V54	P = 0.1223	0.038	0.025	−2.165	1.039	0.990–1.090	P = 0.4676	0.618	0.494–0.732
	V56	P = 0.0448	0.061	0.031	−2.260	1.063	1.001–1.129	P = 0.9545	0.636	0.512–0.747
	V58	P = 0.0367	0.072	0.035	−2.204	1.075	1.004–1.151	P = 0.9999	0.625	0.501–0.738
	V60	P = 0.0408	0.080	0.039	−2.099	1.083	1.003–1.170	P = 0.7426	0.613	0.489–0.727
	V62	P = 0.0335	0.097	0.046	−2.030	1.101	1.007–1.205	P = 0.7580	0.611	0.487–0.726
	V64	P = 0.0251	0.123	0.057	−1.938	1.131	1.011–1.264	P = 0.6743	0.611	0.487–0.726
Multivariable Logistic Regression		Overall Model Fit	Coefficients and Std Errors			Odds Ratios and 95% CL		HL	ROC Analysis	
endpoint: tox G3	Variable	Significant Level	Coefficient	Std. Error	Constant	Odds ratio	95% CI		ROC	95% CL
V54.V56.V56.V58.V60.V62.V64	V64	P = 0.0251	0.123	0.057	−1.938	1.131	1.012–1.264	P = 0.6743	0.611	0.487–0.726
V64.CTV.SEX.AGE	V64	P = 0.0274	0.121	0.057	−1.896	1.1285	1.010–1.261	P = 0.6125	0.614	0.488–0.730

Table 4
Rate of true positive, true negative, false positive and false negative of G2/G3 and G3 endpoints including some selected dosimetric variables significant at univariable logistic regression.

V56 – G2/G3 acute skin toxicities		
cut off V56 = 7.7 cc	< 7.7 cc (29)	> 7.7 cc (41)
no tox (27)	19/29	8/41
tox (43)	10/29	33/41
V64 – G3 acute skin toxicities		
cut off V64 = 2.7 cc	< 2.7 cc (49)	> 2.7 cc (21)
no tox (57)	43/49	14/21
tox (13)	6/49	7/21
V60 – G2/G3 acute skin toxicities		
cut off V60 = 3.3 cc	< 3.3 cc (29)	> 3.3 cc (41)
no tox (27)	19/29	8/41
tox (43)	10/29	33/41
V60 – G3 acute skin toxicities		
cut off V60 = 5.8 cc	< 5.8 cc (43)	> 5.8 cc (27)
no tox (57)	44/49	13/21
tox (13)	5/49	8/21

skin and subcutaneous tissue. When given in conjunction with RT, mitoxantrone, 5-fluorourcil, cyclophosphamide, paclitaxel, docetaxel, and possibly tamoxifen can result in increased cutaneous toxicity. The term 'radiation recall' refers to a particular form of radiation-related drug toxicity: an inflammatory skin reaction of unknown origin that occurs in a previously irradiated body part subsequent to drug administration [41]. Grade 3/4 dermatitis after RT for Head and Neck Cancer is associated with concomitant administration of Cetuximab [14]. In general, the risk and severity of skin reactions are reduced when prophylactic skin care is administrated [42]. In our population, with most patients treated with neo-adjuvant and concomitant chemotherapy without using Cetuximab, no specific independent effect of chemotherapy was observed, although the limited number of patients treated with radiation alone does not permit any definitive indication.

Quantitative data on HNC skin dose-surface/volume response are thus far largely lacking. Some dose-volume constraints were tentatively derived from a recent study by Studer et al. [14], but the results were heavily influenced by the systematic use of bolus ad Cetuximab assumption, which does not represent current practice in most institutions. It emerged that the use of bolus material and skin areas exposed

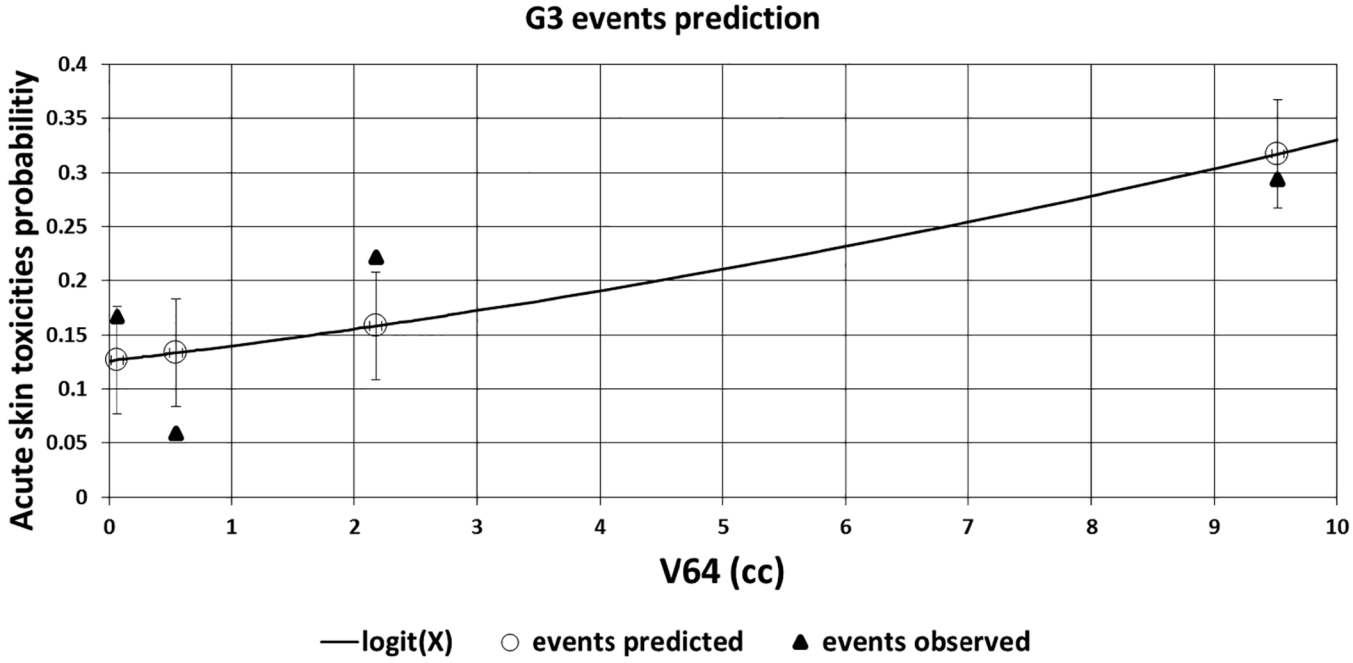

Fig. 7. Logistic plot of the relationship between V64 (resulting as the most predictive DVH parameter) of SL2 and the risk of G3 acute skin toxicity. Triangles show the true rates grouped for each quartile while the circles show the predicted values with their confidence intervals.

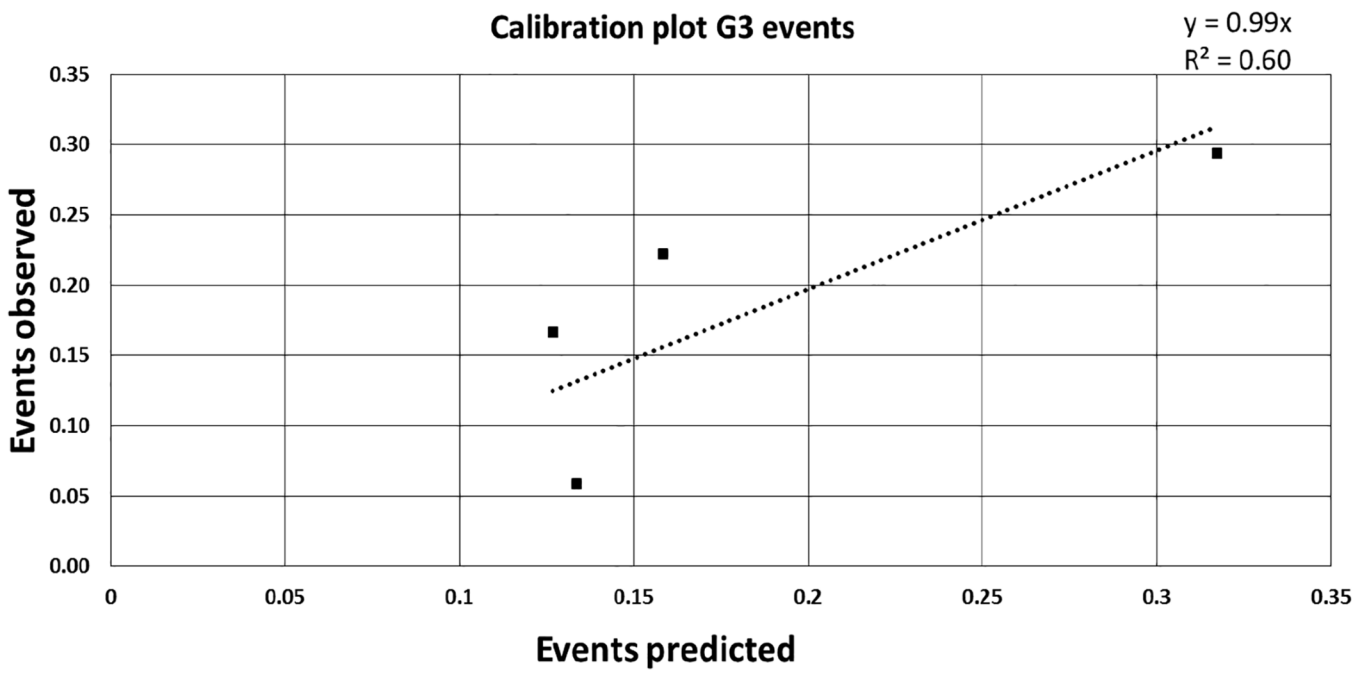

Fig. 8. Calibration plot of the logistic model of Fig. 7 for G3 acute skin toxicity.

to doses > 60 Gy were statistically significantly associated with the development of severe dermatitis in Cetuximab patients, whereas skin areas exposed to > 50 Gy demonstrated a trend towards increased severity of dermatitis. Radaideh et al. [13] studied the effect of skin dose on cutaneous toxicities on a small group of 21 HNC patients. They found that in-vivo measured skin dose > 7 Gy was a risk factor for skin toxicity, implicitly suggesting a relationship between treated volume and severity of effects, similarly to that already observed in the pre-IMRT era and consistent with early findings by Lee at al. [7]. Although skin dose measurement and/or the exploration of more skin-sparing techniques could theoretically be beneficial for HNC patients treated with IMRT, neither clear quantitative data nor robust constraints are available in the literature; this point corroborates the importance of the results reported by our study.

It is important to underline that skin dose is largely influenced by the planning optimization approach in managing the dose within the portion of PTV next to the body contour [43], as well as by the delivery technique. In this context, HT TPS has the exclusive ability to obtain full PTV coverage, even in the top skin layers, by altering the incident fluences in the non-electronic equilibrium region and the planner cannot act to reduce the skin dose in a suitable way.The situation is quite different with other IMRT modalities and TPS systems, where PTV coverage close to the skin can be deliberately reduced by means of various techniques (e.g., skin flash tool, virtual bolus …).

This seems to be the main reason why a higher incidence of skin toxicities developed by patients treated with HT compared to other IMRT techniques [6,8] has been reported. Quite interestingly, our rate of G3 toxicity is consistent with the rate reported by Bibault et al. [8].

Regarding to the accuracy of HT TPS dose calculation in superficial regions, as already stated above, several in vivo and in phantom studies confirmed a good agreement between calculated and measured data, generally within 3–5% [30,31]. There are some other studies, as the one by Avanzo et al. [32], which reported a mean difference of $-6.6\% \pm 2.6\%$ in HN district between calculated and measured in vivo doses with radiochromic EBT films. However, these results should be considered with caution for several reasons. First, measurements in vivo are affected by larger uncertainties due a dependence on detector positioning/inclination in a critical region like the HN and hardly affected by anatomy deformations occurring during treatment [17,44,45]. Interestingly, in a recent study [17] we focused on dose-of-the-day calculation in quantifying changes of skin dose during Tomotherapy for HNC: we found a prevalent skin dose sparing during treatment, explaining results of underdosing reported in vivo by Avanzo et al. and further confirming the accuracy of TPS calculation. Studies using phantoms should be considered to be more reliable: in particular, the study of Zani et al. [30] showed that, when considering radiochromic measurents with films inside the slabs, maximum deviation at the skin level was within 6.5%, reducing to < 3% at 1–2 mm. Due to this and other results [30–32] the choice of considering an uncertainty of 5% (1SD) for SL DVH calculation should be considered very safe; despite this, we verified that dose uncertainty is not expected to have any impact on the found association between DVH shape and toxicity.

In conclusion, the current investigation quantified for the first time the relationship between the planned skin dose (using a 2 mm layer as a surrogate) and the risk of acute cutaneous toxicity in HNC patients treated with SIB (at 2.2 Gy/fr to the high-dose PTV) with Helical Tomotherapy; robust indications regarding dose constraints to limit the risk and the severity of these side effects have been suggested, although they would benefit from prospective confirmation.

Acknowledgments

This work was supported by an AIRC grant (IG18965)

References

[1] Palm A, Johansson K. A review of the impact of photon and proton external beam radiotherapy treatment modalities on the dose distribution in field and out-of-field; implications for the long-term morbidity of cancer survivors. Acta Oncol 2007;46(4):462–73.
[2] Hunter KU, Schipper M, Feng FY, Lyden T, Haxer M, Murdoch-Kinch C-A, et al. Toxicities affecting quality of life after chemo-IMRT of oropharyngeal cancer: prospective study of patient-reported, observer-rated, and objective outcomes. Int J Radiat Oncol Biol Phys 2013;85(4):935–40.
[3] Lohia S, Rajapurkar M, Nguyen SA, Sharma AK, Gillespie MB, Day TA. A comparison of outcomes using intensity-modulated radiation therapy and 3-dimensional conformal radiation therapy in treatment of oropharyngeal cancer. JAMA Otolaryngol – Head Neck Surg 2014;140(4):331–7.
[4] Rosenthal DI, Chambers MS, Fuller CD, et al. Beam path toxicities to non-target structures during intensity-modulated radiation therapy for Head and Neck Cancer. Int l Radiat Oncol Biol Phys 2008;72:747–55.
[5] Kouloulias V, Thalassinou S, Platoni, et al. The treatment outcome and radiation-

induced toxicity for patients with head and neck carcinoma in the IMRT era: a systematic review with dosimetric and clinical parameters. Biomed Res Int 2013:401261.
[6] Al-Mamgani A, Van Rooij P, Verduijn GM, et al. The impact of treatment modality and radiation technique on outcomes and toxicity of patients with locally advanced oropharyngeal cancer. Laryngoscope 2013;123(2):386–93.
[7] Lee N, Chuang C, Quivery JM, et al. Skin toxicity due to IMRT for head and neck carcinoma. Int J Radiation Oncol Biol Phys 2002;53(3):630–7.
[8] Bibault JE, Dussart S, Clinical Giraud P, et al. Outcomes of several IMRT techniques for patients with Head and Neck Cancer: a propensity score-weighted analysis 5 Int J Radiat Oncol Biol Phys 2017;99(4):929–37.
[9] Nevens F, Duprez S, Nuyts, et al. Radiotherapy induced dermatitis is a strong predictor for late fibrosis in Head and Neck Cancer. The development of predictive model for late fibrosis. Radiother Oncol 2017;122:212–7.
[10] Turesson I, Thames HD. Repair capacity and kinetics of human skin during fractionated radiotherapy: erythema, desquamation, and telangiectasia After 3 and 5 year's follow-up. Radiother Oncol 1989;15:169–88.
[11] Bray FN, Simmons BJ, Wolfson AH, et al. Acute and chronic cutaneous reactions to ionizing radiation Therapy. Dermatol Ther(Heidelb) 2016;6(2):185–206.
[12] Bonomo P, Loi M, Desideri I, et al. Incidence of skin toxicity in squamous cell carcinoma of the head and neck treated with radiotherapy and cetuximab: a systematic review. Crit Rev Oncol/Hematol 2017;120:98–110.
[13] Radaideh KM, Matalqah LM. Predictors of radiation-induced skin toxicity in nasopharyngeal cancer patients treated by intensity-modulated radiation therapy: a prospective study. J Radiother Pract 2016;15(3):276–82.
[14] Studer G, Brown M, Glanzmann C, et al. Grade 3/4 dermatitis in Head and Neck Cancer patients treated with concurrent cetuximab and imrt. Radiat Oncol Biol Phys 2011;81:110–7.
[15] Branchini M, Fiorino C, Broggi S, et al. Validation of a method for “dose of the day” calculation in head-neck Tomotherapy by using planning CT-to-MVCT deformable image registration. Phys Med 2017;39:73–9.
[16] Branchini M, Broggi S, Dell’Oca I, et al. Skin dose calculation during radiotherapy of head and neck cancer using deformable image registration of planning and megavoltage computed tomography scans. Phiro 2018;8:44–50.
[17] Mori M, Branchini M, Broggi S et al. Quantification of skin dose changes during Tomotherapy for head-neck cancer by dose-of-the-day recalculation. Oral Presentation at AIFM 10, 2018 Bari.
[18] Von Essen CF. A spatial model of time-dose-area relationships in radiation therapy. Radiology 1963;81:881–3.
[19] Fu HJ, Li CW, Tsai WT, et al. Skin dose for Head and Neck Cancer patients treated with intensity-modulated radiation therapy (IMRT) 2017. Radiat Phys Chem 2017;140:435–41.
[20] Merlotti A, Alterio D, Vignataglianti R, et al. Technical guidelines for Head and Neck Cancer IMRT on behalf of the Italian association of radiation oncology – head and neck working group. Radiat Oncol 2014;9:264.
[21] Widesott L, Pierelli A, Fiorino C, et al. Intensity-modulated proton therapy versus helical tomotherapy in nasopharynx cancer: planning comparison and NTCP evaluation. Int J Radiat Oncol Biol Phys 2008;72(2):589–96.
[22] Fiorino C, Dell'Oca I, Pierelli A, et al. Simultaneous integrated boost (SIB) for nasopharynx cancer with helical tomotherapy, a planning study. Strahlenther Onkol 2007.
[23] Gregoire V, Levendag P, Ang KK, et al. CT-based delineation of lymph node levels and related CTVs in the node-negative neck: DAHANCA, EORTC, GORTEC, NCIC RTOG consen- sus guidelines. Radiother Oncol 2003;69:227–36.
[24] RTOG H-0022. Phase I/II study of conformal and intensity modulated irradiation for oropharyngeal cancer. http://www.rtog.org/members/protocols/h0022/h0022.pdf [Accessed January, 2008].
[25] Eisbruch A, Ten Haken RK, Kim HM, et al. Dose, volume and function relationships in parotid salivary glands following con- formal and intensity-modulated irradiation of Head and Neck Cancer. Int J Radiat Oncol Biol Phys 1999;45:577–87.
[26] Fiorino C, Dell’Oca I, Broggi S, et al. Significant improvement in normal tissue sparing and target coverage for Head and Neck Cancer by means of helical tomotherapy. Radiother Oncol 2006;78:276–82.
[27] Edge SB, Compton CC. The American Joint Committee on Cancer: the 7th edition of the AJCC cancer staging manual and the future of TNM. Ann Surg Oncol 2010;17:1471–4.
[28] Sterpin E, Salvat F, Olivera G, et al. Monte Carlo evaluation of the convolution/superposition algorithm of Hi-Art™ tomotherapy in heterogeneous phantoms and clinical cases. Med Phys 2009;36:1566–75.
[29] Zhao Y, Mackenzie M, Kirby C, Fallone BG. Monte Carlo evaluation of a treatment planning system for helical tomotherapy in an anthropomorphic heterogeneous phantom and for clinical treatment plans. Med Phys 2008;35:5366–74.
[30] Zani M, Talamonti C, Pallotta S, et al. In phantom assessment of superficial doses under TomoTherapy irradiation. Phys Med 2016;32:1263–70.
[31] Tournel K, Verellen D, Storme G, et al. An assessment of the use of skin flashes in helical tomotherapy using phantom and in-vivo dosimetry. Radiother Oncol 2007;84:34–9.
[32] Avanzo M, Drigo A, Ren Kaiser S, et al. Dose to the skin in helical tomotherapy: results of *in vivo* measurements with radiochromic films. Phys Med 2013;29(3):304–11.
[33] Hopewell JW. The skin: its structure and response to ionizing radiation. Int J Radiat Oncol Biol Phys 1990;57(4):751–73.
[34] Archambeau JO, Pezner R, Wasserman T. Pathophysiology of Irradiated Skin and Breast. Int J Radiat Oncol Biol Phys 1995;31(5):1171–85.
[35] Common Terminology Criteria for Averse Events v4.0 (CTCAE). https://www.eortc.be/services/doc/ctc/CTCAE_4.03_2010-06-14_QuickReference_5x7.pdf.
[36] Sini C, Noris Chiorda B, Gabriele P, et al. Patient-reported intestinal toxicity from whole pelvis intensity-modulated radiotherapy: first quantification of bowel dose–volume effects. Radiother Oncol 2017;124:296–301.
[37] Hosmer DW, Lemeshow S. Goodness of fit tests for the multiple logistic regression model. Commun Stat Theor Meth 1980;9:1043–69. https://doi.org/10.1080/03610928008827941.
[38] Pastore F, Conson M, D'Avino V, et al. Dose-surface analysis for prediction of severe acute radio-induced skin toxicity in breast cancer patients. Acta Oncol 2016;55(4):466–73.
[39] Jagsi R, Griffith KA, Boike TP, et al. Differences in the acute toxic effects of breast radiotherapy by fractionation schedule: comparative analysis of physician-assessed and patient-reported outcomes in a large multicenter cohort. JAMA Oncol 2015;1(7):918–30.
[40] Lilla C, Ambrosone CB, Kropp S, et al. Predictive factors for late normal tissue complications following radiotherapy for breast cancer. Breast Cancer Res Treat 2007;106(1):143–50.
[41] Balter S, Hopewell JW, Donald L, et al. Fluoroscopically guided interventional procedures: a review of radiation effects on patients’ skin and hair. Radiology 2010;254(2):326–41.
[42] Chen MF, Chen WC, Lai CH, et al. Predictive factors of radiation-induced skin toxicity in breast cancer patients. BMC Cancer 2010;10. 508-2407-10-508.
[43] Sick J, Fontenot J. The air out there: treatment planning when target volumes extend beyond the skin. Int J Radiat Oncol Biol Phys 2018;101(5):1025–6.
[44] Cilla S, Meluccio D, Fidanzio A, et al. Initial clinical experience with Epid-based in-vivo dosimetry for VMAT treatments of head-and-neck tumors. Phys. Med. 2016;32(1):52–8.
[45] Tachibana H, Motegi K, Moriya S. Impact of shoulder deformation on volumetric modulated arc therapy doses for Head and Neck Cancer. Phys Med 2018;53:118–28.